Geomorphology 337 (2019) 79–93

Contents lists available at ScienceDirect

Geomorphology

journal homepage: www.elsevier.com/locate/geomorph

Early Holocene slope erosion in the Scheldt basin (Belgium): Naturally and/or human induced?

Philippe Crombé [a,*], Annelies Storme [b], Frédéric Cruz [c], Luc Allemeersch [c], Hans Vandendriessche [a], Koen Deforce [a,d], Jari Mikkelsen [c], Kim Aluwé [c], Mathieu Boudin [e], Joris Sergant [c]

[a] Ghent University, Department of Archaeology, Sint-Pietersnieuwstraat 35, B-9000 Gent, Belgium
[b] Ghent University, Department of Geology, Krijgslaan 281 - S8, B-9000 Gent, Belgium
[c] Gate bvba, Dorpstraat 73, B-8450 Bredene, Belgium
[d] Royal Belgian Institute of Natural Sciences, Vautierstraat 29, B-1000 Brussels, Belgium
[e] Royal Institute for Cultural Heritage, Jubelpark 1, B-1000 Brussels, Belgium

ARTICLE INFO

Article history:
Received 5 December 2018
Received in revised form 20 March 2019
Accepted 25 March 2019
Available online 30 March 2019

Keywords:
Slope erosion
Early Holocene
Forest fires
Prehistoric hunter-gatherers
Levee

ABSTRACT

The last decade increasing evidence of soil erosion by sediment run-off predating agriculture has been found in different areas of west and central Europe. A central discussion is whether pre-agricultural erosion was triggered by vegetational disturbances caused by hunter-gatherer activities (trampling, controlled forest fires) or natural processes (e.g. climatic anomalies, wildfires, wind-throws). This paper contributes to this discussion using data recently gathered during archaeological excavations of a levee, within the floodplain of the River Scheldt in NW Belgium, occupied by hunter-gatherers during the Early Holocene. These excavations revealed the presence of a ca. 40 cm thick slope deposit, which was radiocarbon dated to the late Preboreal and 1st half of the Boreal. A high-resolution, multi-proxy analysis of this deposit demonstrates a close correlation between the type of vegetation, forest fires and erosion intensity. It is concluded that repeated burning of pine-dominated forests was most likely the main trigger. Furthermore, this study provides strong evidence against an anthropogenic origin of these Early Holocene fires as burning and slope erosion already started long before prehistoric hunter-gatherers occupied the levee top and the Scheldt basin. Furthermore, this study demonstrates that pre-agricultural slope erosion was not limited to hilly regions with pronounced topography but also occurred in lowland regions with subtle topographical gradients.
© 2019 The Authors. Published by Elsevier B.V. This is an open access article under the CC BY-NC-ND license (http://creativecommons.org/licenses/by-nc-nd/4.0/).

1. Introduction

It is generally assumed that soil erosion started when man began to cut down the forest and cultivate the soil for agro-pastoral purposes (Kalis et al., 2003; Notebaert et al., 2011), that is at the start of the Neolithic at its earliest (in Europe locally varying between 8000 and 6000 cal BP). However, the last few years increasing evidence of pre-agricultural erosion has been gathered, dating to the period in which the environment was exploited by small bands of migrating hunter-gatherer-fishermen. Tolksdorf and Kaiser (2012) and Sevink et al. (2018) recently reported aeolian activity dating to the Early Holocene within the European sand-belt. Dreibrodt et al. (2010a, 2010b) and Hoffmann et al. (2008) on the other hand documented Early Holocene slope erosion by water at several mid-latitude locations all over Germany.

A central discussion in these studies is the question about the possible causes of pre-agricultural erosion. Besides very local triggers, such as game browsing, human and animal trampling and wind-throws, most of the aforementioned studies link soil instability with repeated forest fires. This is often based on the presence of embedded macro- and/or microcharcoal. These forest fires created openings with little or no undergrowth, which were very vulnerable to erosion either by wind or water runoff. Whether these fires were naturally induced (wildfires caused by lightning) or intentionally ignited by prehistoric hunter-gatherers is another point of debate. However, this debate is generally hampered by insufficient proof of contemporaneous human activity in the vicinity of these palaeofires, especially for the Early Holocene.

The site of Kerkhove (NW Belgium) in the Middle-Scheldt floodplain offers the unique occasion to investigate the relationship between humans, forest fires and erosion during the Early Holocene. Archaeological excavations conducted in 2015–2016 at this site revealed a colluvial deposit at the foot of a Lateglacial levee. A multiproxy analysis allowed for a detailed characterization of this deposit, using pollen, plant

* Corresponding author.
E-mail addresses: philippe.crombe@ugent.be (P. Crombé), annelies.storme@ugent.be (A. Storme), fredericcruz@hotmail.com (F. Cruz), allemeersch.luc@skynet.be (L. Allemeersch), Hans.vandendriessche@ugent.be (H. Vandendriessche), koen.deforce@ugent.be, koen.deforce@naturalsciences.be (K. Deforce), jari.mikkelsen@telenet.be (J. Mikkelsen), kim.aluwe@outlook.be (K. Aluwé), Mathieu.boudin@kikirpa.be (M. Boudin), joris.sergant@gatearchaeology.be (J. Sergant).

https://doi.org/10.1016/j.geomorph.2019.03.025
0169-555X/© 2019 The Authors. Published by Elsevier B.V. This is an open access article under the CC BY-NC-ND license (http://creativecommons.org/licenses/by-nc-nd/4.0/).

macroremains, microscopic and macroscopic charcoal fragments, loss-on-ignition (LOI), micromorphology and grain-size analysis. The top of the levee on the other hand yielded evidence of repeated occupation by Mesolithic hunter-gatherers from the Early to Middle Holocene. A large series of radiocarbon dates allows to correlate the environmental and archaeological evidence in order to investigate the possible synchronicity between forest fires, slope erosion, human occupation and climatic events.

2. Materials and methods

2.1. Site description

Kerkhove is situated in a hilly area of NW Belgium, called "the Flemish Ardennes" (Fig. 1). The area is dominated by Paleogene hills (max. height 156 m TAW = Belgian ordnance level, corresponding to −2.3 MSL) covered with (sandy) loam sediments mainly dating to the Weichselian. The site of Kerkhove is situated in the Lateglacial floodplain of the middle reaches of the river Scheldt, on an extensive NE-SW oriented sandy levee (length > 550 m; mean width c. 80 m; mean height 3 m) covered by several meters of Holocene peat and alluvial clay. Thanks to this thick cover, the archaeological sites excavated on top of the levee are well-preserved. During the Early Holocene the levee was flanked at both long sides by natural depressions (Fig. 1): to the north by a shallow depression later filled with peat, and to the south by a c. 8 m deep palaeochannel of the Scheldt, which has been partially eroded by the actual Scheldt river. The evidence of colluvial deposits was discovered along the southern foot of the levee, which is characterized by a slope ranging between c. 12° and 16°.

2.2. Field methods

The levee at Kerkhove was excavated over a surface of c. 5000 m^2. After mechanical removal of the covering alluvial clay and peat, excavations started with the systematic wet sieving of the levee top in a ¼ m^2 grid, to collect settlement waste (lithic artefacts, charred plant macroremains and animal bones) from the Mesolithic occupations. Subsequently the steep slope towards the palaeochannel was investigated by means of 4 long and deep transects (T1-T4) which were mechanically excavated, providing 4 cross-sections of the levee from top to base (Fig. 1). The profiles of these transects were registered in detail and used for multi-proxy palaeoenvironmental sampling.

2.3. Laboratory methods

The colluvial layer was best preserved in transects 1 (T1) and 3 (T3) (Fig. 2; unit VII); hence these profiles have been selected for multi-proxy environmental analysis.

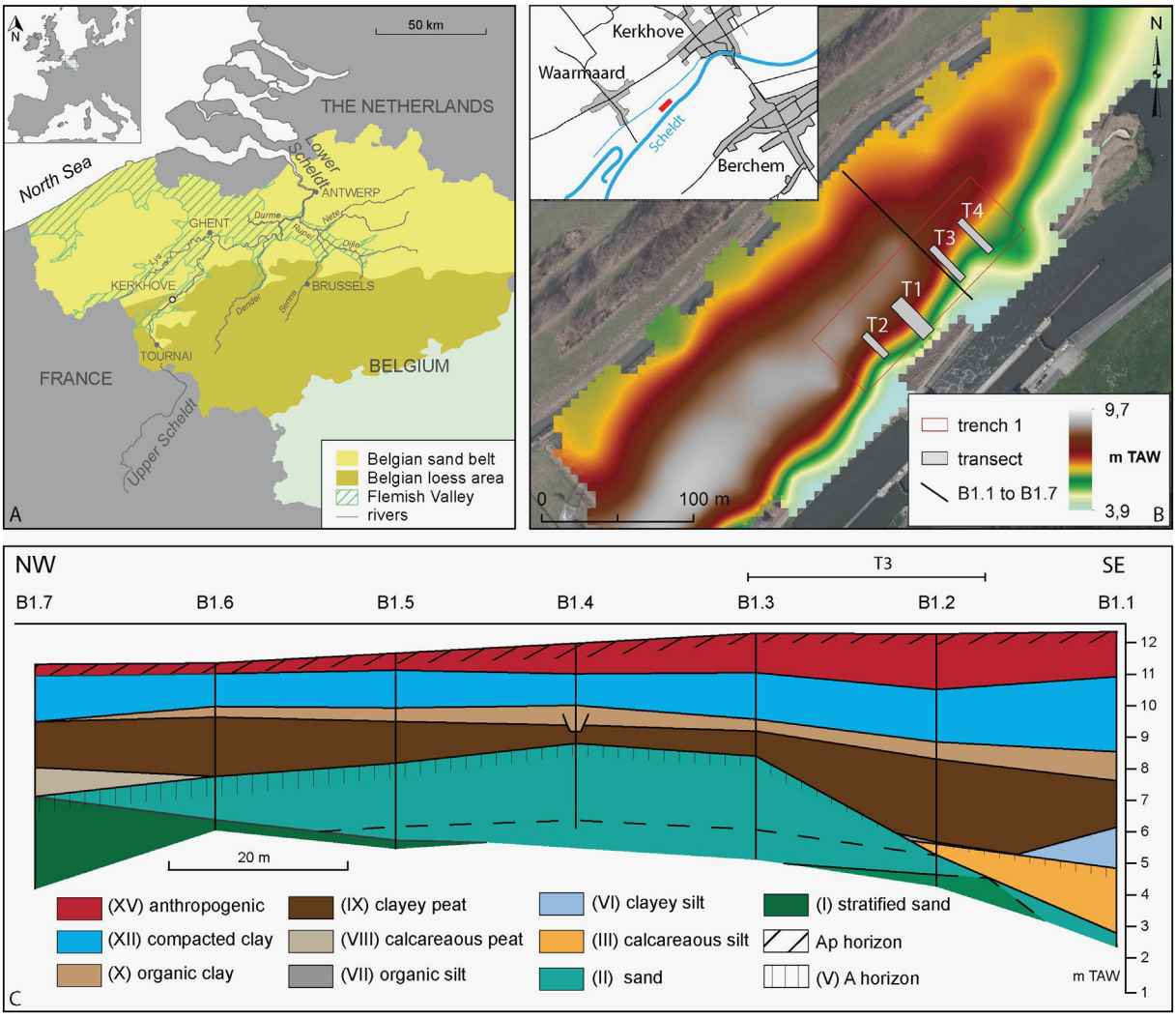

Fig. 1. Top left: Location of the site of Kerkhove within Europe and Belgium; Top right: Topography of the covered levee at Kerkhove with the position of trench 1 and its stratigraphical transects (T1-T4) and the mechanical coring transect (B1.1-B1.7); Bottom: transect of the levee and adjacent depressions based on the mechanical coring data.

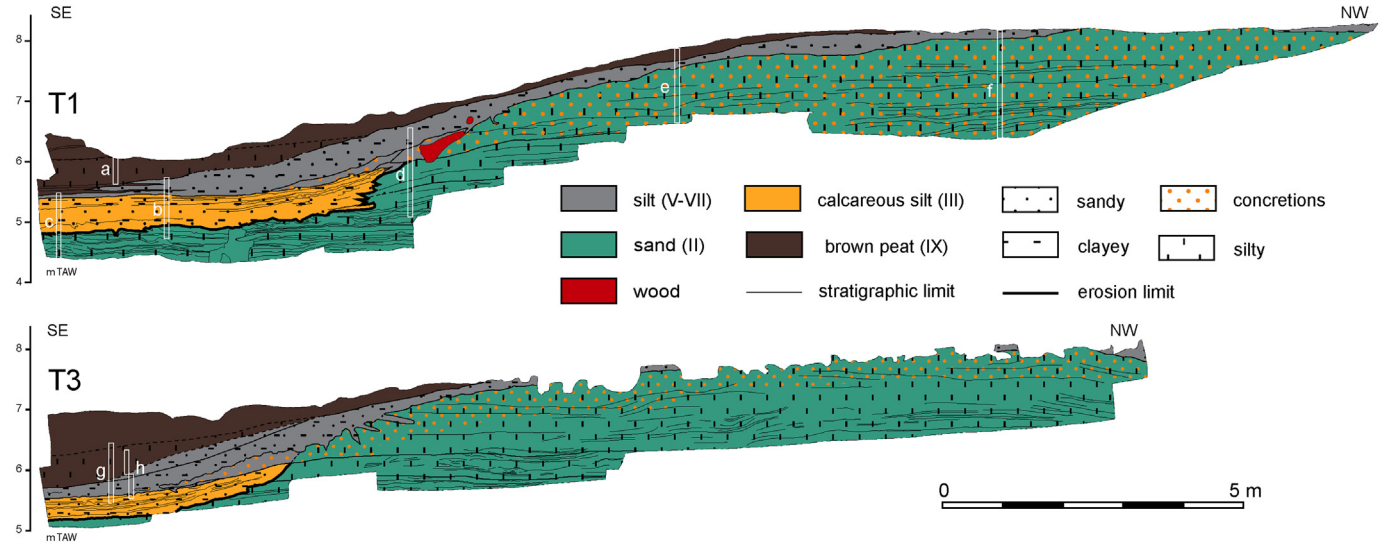

Fig. 2. Lithostratigraphical section of T1 (top) and T3 (bottom) with indication of the sampling locations (a-g) for sedimentological analyses. The above-lying peat (top IX and X) and alluvial clay deposits (XII) were already removed mechanically before the excavation of the transects.

2.3.1. Lithological description

All transect profiles have been studied macroscopically in the field using different parameters, such as (1) lithology (colour and grain-size determination), (2) sedimentological features and post-depositional deformation, (3) thickness and bed form and (4) character of lower and upper boundaries of sediment beds (transitional, sharp or erosional) and presence of internal erosional surfaces. The registration was done by means of photogrammetry and georeferencing.

2.3.2. Loss-on-ignition and grain-size analysis

Sampling for loss-on-ignition (LOI) and grain-size analysis followed an 8 cm interval. Analysis was done according to the protocol proposed by Heiri et al. (2001) for LOI and Mulitza et al. (2008) for grain-size. The grain sizes concerned the range from 0.1 to 3500 μm. The terminology follows Folk (1954) and the statistical parameters of Folk and Ward (1957).

2.3.3. Micromorphology

For micromorphological research, undisturbed samples of the different layers were collected in metal boxes. The dried samples were embedded with resin to fill pores and fix soil particles. Progressive thinning and polishing resulted in the standard thickness of 30 μm. Thin sections were studied using a polarizing microscope with normal or plane polarized light (PPL), crossed polarized light (XPL) or oblique incident light (OIL). The description is done according to the terminology and concepts of Stoops (2003).

2.3.4. Palynological and microcharcoal analysis

In T3 the succession was studied at high resolution, with 2 cm intervals between samples. The subsamples of c. 1.0 cm^3 were treated by standard techniques for palynological preparation (Moore et al., 1991). The residues were studied using a light microscope at 400× magnification and identification of all palynomorphs was pursued, including pollen (Beug, 2004), spores (Moore et al., 1991) and non-pollen palynomorphs (NPP; van Geel, 1978; van Geel et al., 1981, 1983, 1989; Bakker and Van Smeerdijk, 1982). In the intervals of interest, a pollen sum of c. 400 was counted, including all pollen of terrestrial plants (arboreal pollen; AP) and non-arboreal pollen (NAP). All palynomorphs were counted and expressed as percentages of the pollen sum. Preservation condition was assessed and rated between 1 (very poor) and 5 (excellent). Pollen concentration was calculated by adding a known amount of *Lycopodium* spores and defining the ratio of counted *Lycopodium* to pollen sum (Stockmarr, 1971). Finally, local pollen biozones were defined and linked to regional biozones described for the Scheldt basin (Storme et al., 2017).

Microcharcoal concentration was calculated based on a count of c. 200 particles. All elements were presented in a pollen diagram, using Tilia software (Grimm, 2015). Due to the use of centrifuge and vortex during preparation, which possibly caused further fragmentation of charcoal, size measurements of the charcoal fragments, in order to make a distinction between local and regional fires, were not useful. Hence the microcharcoal counts need to be regarded as a general relative estimate of overall fire activity in the region.

2.3.5. Plant macroremains

Samples of 1000 cm^3 for the analysis of plant macroremains were continuously collected from the studied profile of T3. The samples were sieved with meshes of 2 mm and 500 μm with water under low pressure. A stereoscopic binocular microscope at 10× to 45× magnification was used for taxonomic identifications, which is based on Cappers et al. (2006). Most of the identified plant macroremains, placed in general ecological groups, are presented in a diagram, using Tilia software (Grimm, 2015).

2.3.6. Macrocharcoal analysis

Charcoal fragments were carefully selected from the sieved 2 mm residues that were also used for the analysis of the other botanical macroremains, using a stereo lens. The charcoal fragments were air-dried for one week and studied using a metallographic microscope with incident dark-field illumination and magnifications between 50× and 500×. Identifications are based on Schweingruber (1990) and Schoch et al. (2004) and the anthracological reference collection of the Royal Belgian Institute of Natural Sciences (Brussels).

2.3.7. Archaeological analysis

The sieved archaeological remains from the levee top mainly consist of lithic artefacts (tools and production waste) and faunal remains. The study of the lithics comprises three aspects: 1° a typo-technological analysis of all artefacts (N = c. 56,500), mainly for relative dating purposes (e.g. Crombé et al., 2009); 2° a spatial analysis using density maps and 3° a taphonomic analysis (e.g. Villa, 1982; Collcutt et al., 1990; Hoffman, 1992) and palaeoethnographic reconstruction of the Mesolithic occupation(s) by means of refitting (e.g. Leroi-Gourhan and Brézillon, 1972; Cahen et al., 1979). The latter involves the joining together of lithic artefacts in view of reconstructing the original nodules.

2.3.8. Radiocarbon dating

2.3.8.1. Palaeoenvironmental dating

2.3.8.1.1. Sample selection and dating. Sampling for radiocarbon dating was mainly done stratigraphically on the vertical section of T3 and to a much lesser extend to T1. Depending on the thickness of the lithostratigraphic units, several samples (mean thickness 2 cm) were taken per unit, so that at least the basis and top of each could be dated. Dating was mainly performed on unburnt terrestrial plant macroremains, and to a lesser extent on carbonized plant remains, such as charred hazelnut shells, or on bulk soil samples (Table 1). The latter were used when terrestrial plant macroremains were lacking.

All samples were pretreated with the standard AAA-method (HCl-NaOH-HCl, all 1%). Pretreated bulk soil samples were transferred into quartz tubes with CuO and Ag and combusted to CO_2 at 400 °C. A combustion temperature of 400 °C was chosen to minimize the contribution of the more refractory carbon bound to clay minerals in the sample (McGeehin et al., 2001, 2004). Graphitization of CO_2 was carried out using H_2 over a Fe catalyst. Most samples were AMS-dated at the Royal Institute for Cultural Heritage, Brussels (Belgium) (Van Strydonck and Van der Borg, 1990–1991), except for the smallest samples (< 10 mg C); these were dated by means of Gas Ion Source dating at ETH-Zürich (Switzerland) (Hajdas, 2008; Ruff et al., 2010).

2.3.8.1.2. Modelling of radiocarbon dates. The modelling of the radiocarbon dates was performed using Bayesian statistics (Bronk Ramsey, 2009), available from the online OxCal program version v4.3. All dates were calibrated according to the IntCal13 atmospheric calibration curve (Reimer et al., 2013). Bayesian modelling was done using the "Sequence" function, allowing to calculate the start and end of each lithostratigraphic unit. The Agreement Index was used for selecting the most reliable dates; dates with an Agreement Index below 60% were considered as outliers and eliminated from the model (Bronk Ramsey, 1995).

2.3.8.2. Archaeological dating. In order to date the human occupation on the levee top, 16 single-entity samples of charred hazelnut shells were AMS-dated in Brussels. These were selected from the center of presumed surface-hearths, following the guidelines of Crombé et al. (2013). The latter however were only clearly observed within Early Mesolithic loci; hence it was not possible to date the Middle Mesolithic occupation of the site. Attempts to use uncalcined animal bone to solve this dating problem failed due to insufficient collagen, except for one sample, i.e. a wild boar premolar (Table 3).

The archaeological dates were further processed using the "Phase" function within the Bayesian modelling package of OxCal. This enabled us to define the start and end date of the Early Mesolithic occupation, which most likely consisted of several, temporal (seasonal) occupation events.

Table 2
Results of the Bayesian modelling of the start and end of each lithostratigraphic unit in T3 and the Mesolithic occupation.

	68.2% Probability		95.4% Probability	
	Cal BP		Cal BP	
	Start	End	Start	End
Unit IX (lower half)	9675–9550	8162–7883	9781–9546	8174–7370
Unit VII	11,389-11,192	9850–9697	11,808-11,181	9882–9613
Mesolithic occupation	10,630-10,492	9684–9532	10,739-10,433	9845–9415

3. Results

3.1. Lithostratigraphy and sediment analysis

Based on the field descriptions 18 lithostratigraphic units were identified on the level of the entire site (cf. Supplementary data Table 1). In this paper just 5 units will be discussed in detail (Figs. 2, 3).

Unit II: bluish grey, reduced to brownish grey oxidized silty sand with silty and clayey stratification. According to the sediment analysis this unit can be classified as poorly sorted silty sand with a very low carbonate and organic component (mean $CaCO_3$: 5.9%; mean OM: 1.4%). The grain-size presents an important vertical variability, except for the

Table 1
List of palaeoenvironmental and archaeological ^{14}C dates from the slope deposit (VII) and the peat (IX) at the foot of the levee along the palaeochannel of the Scheldt (T3). Dates in italic are considered outliers according to the Bayesian model (Agreement Index <60%).

ID	Unit	From	To	Mean	Sample composition	Lab code	Date
		Depth (m TAW)					Uncal BP
Palaeoenvironmental samples							
VN 2290	IX	6,72	6,70	6,68	*Mentha* cf. *aquatica* (13), *Urtica dioica* (25 and 2 fragm.), *Oenanthe* sp. (1 fragm.), *Lemna* (1), *Chenopodium album* (1)	RICH-25344	7311 ± 41
VN 2290	IX	6,43	6,41	6,42	*Mentha* cf. *aquatica* (5)	*ETH-84514*	*7825 ± 42*
VN 2289	IX	6,27	6,25	6,26	*Mentha* cf. *aquatica (1), Urtica dioica (2), Lemna (1)*	*ETH-84515*	*7537 ± 95*
VN 2289	IX	6,25	6,23	6,24	*Mentha* cf. *aquatica* (5), *Urtica dioica* (1), *Oenanthe* sp. (1 fragm.)	ETH-84516	8147 ± 46
VN 3229	IX	6,15	6,13	6,14	*Galeopsis*	*RICH-22538*	*8479 ± 38*
VN 3233	IX	6,07	6,05	6,06	*Urtica - Galeopsis*	RICH-22539	8351 ± 40
VN 2289	IX	6,05	6,03	6,04	*Mentha* cf. *aquatica* (4), *Urtica dioica* (2)	ETH-84517	8615 ± 81
VN 2289	IX	6,01	5,99	6,00	*Lemna* sp. (2), *Chenopodium* sp. (1), charred hazelnut shell	RICH-25346	8628 ± 40
VN 3383	VII	5,99	5,96	5975	charred hazelnut shell	*RICH-25339*	*9049 ± 39*
VN 3383	VII	5,99	5,96	5975	*Mentha* cf. *aquatica* (5), *Urtica dioica* (1), *Lemna sp.* (1)	*ETH-84520*	*8633 ± 85*
VN 3383	VII	5,96	5,93	5945	*Mentha* cf. *aquatica* (1), *Urtica dioica* (8), Galeopsis (1 fragm), Alismataceae (1)	*ETH-84518*	*8659 ± 83*
VN 3383	VII	5,90	5,87	5885	charred hazelnut shell	*RICH-25338*	*8975 ± 38*
VN 3383	VII	5,90	5,87	5885	*Mentha* cf. *aquatica* (1 fragm.), *Urtica dioica* (2 and 1 fragm.)	ETH-84521	8797 ± 166
VN 2290C	VII	5,86	5,85	5855	soil bulk	RICH-22504	8967 ± 43
VN 3244	VII	5,85	5,83	5,84	charred hazelnut shell	*RICH-22540*	*9282 ± 43*
VN 3244	VII	5,85	5,83	5,84	*Sambucus* sp.	RICH-22495	9175 ± 41
VN 3383	VII	5,78	5,75	5765	*Mentha* cf. *aquatica* (2), *Urtica dioica* (2), *Chenopodium album* (1 fragm.), *Galeopsis* sp. (2 fragm.), charred hazelnut shell	RICH-25345	9303 ± 38
VN 2290 B	VII	5,74	5,73	*5735*	soil bulk	RICH-22501	9292 ± 41
VN 2290 A	VII	5,62	5,61	*5615*	soil bulk	RICH-22497	9750 ± 44
Archaeological samples							
126081	VII				fragment of tibia wild boar	RICH-22498	8823 ± 41
126862	VII				fragment of scapula deer	RICH-22499	8304 ± 40
126380	VII				charred hazelnut shell	RICH-22494	9239 ± 43
126586	VII				charred hazelnut shell	RICH-22503	9145 ± 44

Table 3
List of radiocarbon dates related to the Mesolithic occupation on the top of the levee.

ID	Lithic locus	Sample composition	Lab code	Date	%
				Uncal BP	Agreement index
144220	off-site	teeth wild boar	RICH-24377	6222 ± 35	
284316	10	charred hazelnut shell	RICH-23842	8671 ± 34	71
181996	6	charred hazelnut shell	RICH-23838	8796 ± 40	101
181085	6	charred hazelnut shell	RICH-23841	8803 ± 38	100
143635	1b	charred hazelnut shell	RICH-23847	8859 ± 35	100
273087	11	charred hazelnut shell	RICH-23839	8860 ± 37	100
265852	10	charred hazelnut shell	RICH-25190	8884 ± 37	100
153703	2	charred hazelnut shell	RICH-23846	8916 ± 35	100
263224	12	charred hazelnut shell	RICH-25196	8921 ± 36	100
265842	10	charred hazelnut shell	RICH-25195	8989 ± 35	100
264898	10	charred hazelnut shell	RICH-23848	9132 ± 35	100
174705	3	charred hazelnut shell	RICH-24385	9136 ± 40	100
264098	10	charred hazelnut shell	RICH-23840	9156 ± 34	100
265887	10	charred hazelnut shell	RICH-24671	9224 ± 42	101
265777	10	charred hazelnut shell	RICH-24673	9275 ± 42	101
265196	10	charred hazelnut shell	RICH-24672	9303 ± 43	97
275595	10	charred hazelnut shell	RICH-24670	9320 ± 41	93

upper 1 m which is very homogenous. The latter is also characterized by a higher $CaCO_3$ amount. This unit constitutes the levee.

Unit III: brown grey to pale brown calcareous, organic-rich silt with gastropod shells interstratified with sandy to silty layers. Due to bioturbation the top of this unit is locally strongly homogenized. The analysis points to a poorly sorted, sandy very coarse silt with a low OM content (mean 4.2%) and higher $CaCO_3$ content (mean 13.0%). This unit is interpreted as a lacustrine deposit, with seasonal fluvial influence.

Unit V: sandy sediment with organic silt presenting a strong lateral variation. Situated above unit III it is characterized as a 5 to 10 cm thick, black layer of silty clay and sand. The limit can be abrupt or gradual. Situated above unit II it rather consists of a 20 to 40 cm thick, blackish layer with a texture closely resembling the underlying layer. Locally this layer is covered by a 5 cm thick silty clay which is difficult to distinguish from the above-lying peat. Very locally biogalleries and tree-fall features occur at the base of unit V, indicating activities of burrowing animals and plants. Finally, the presence of numerous iron-manganese concretions needs to be mentioned.

Based on the sediment analyses this unit consists of poorly sorted, silty very fine sand to sandy very coarse silt, with a high amount of

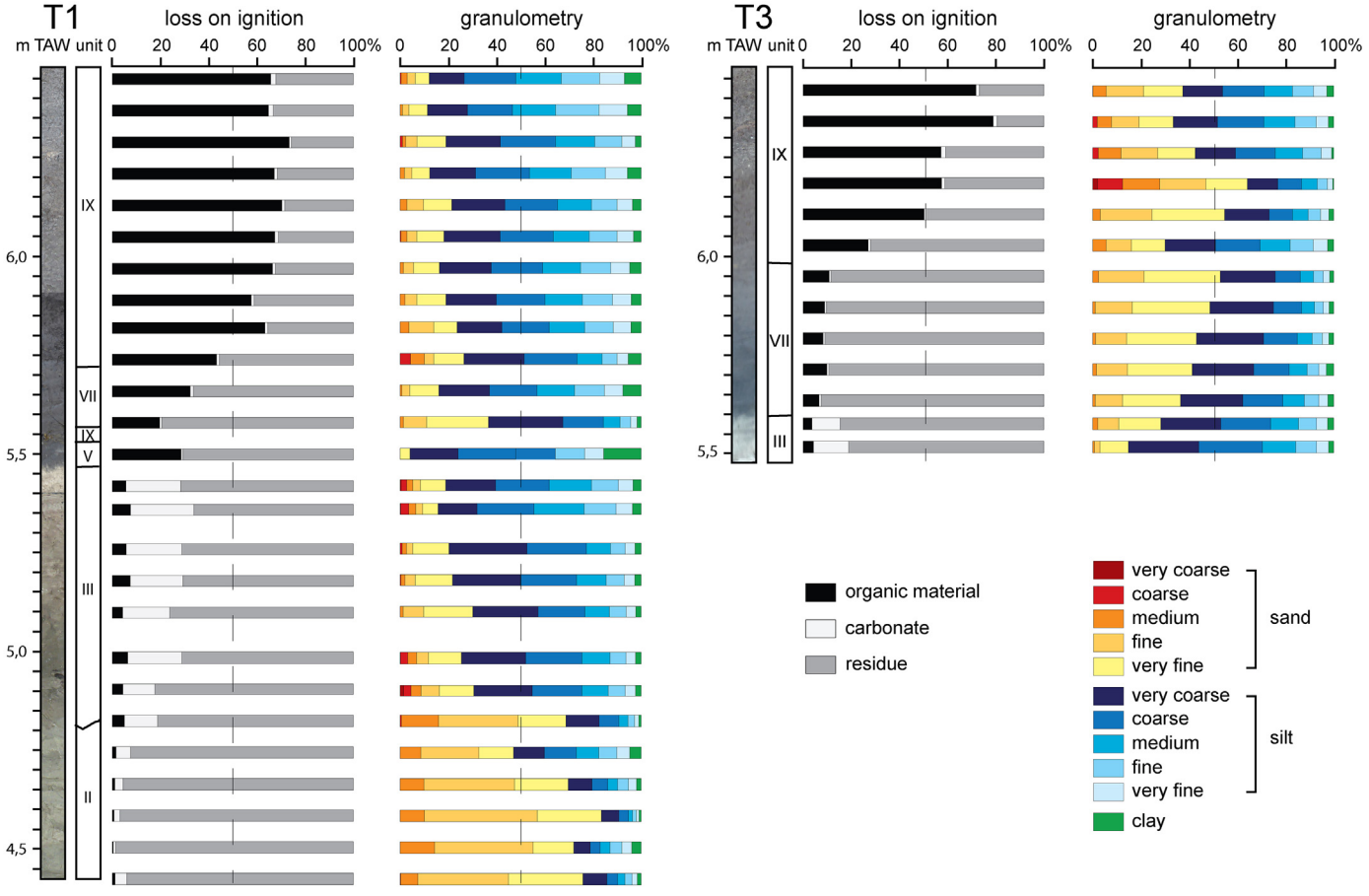

Fig. 3. Sediment analysis of T1 (locations a, b and c in Fig. 2) and T3 (location g in Fig. 2). The slightly, very fine gravelly fraction (<1%) from a unique sample not considered.

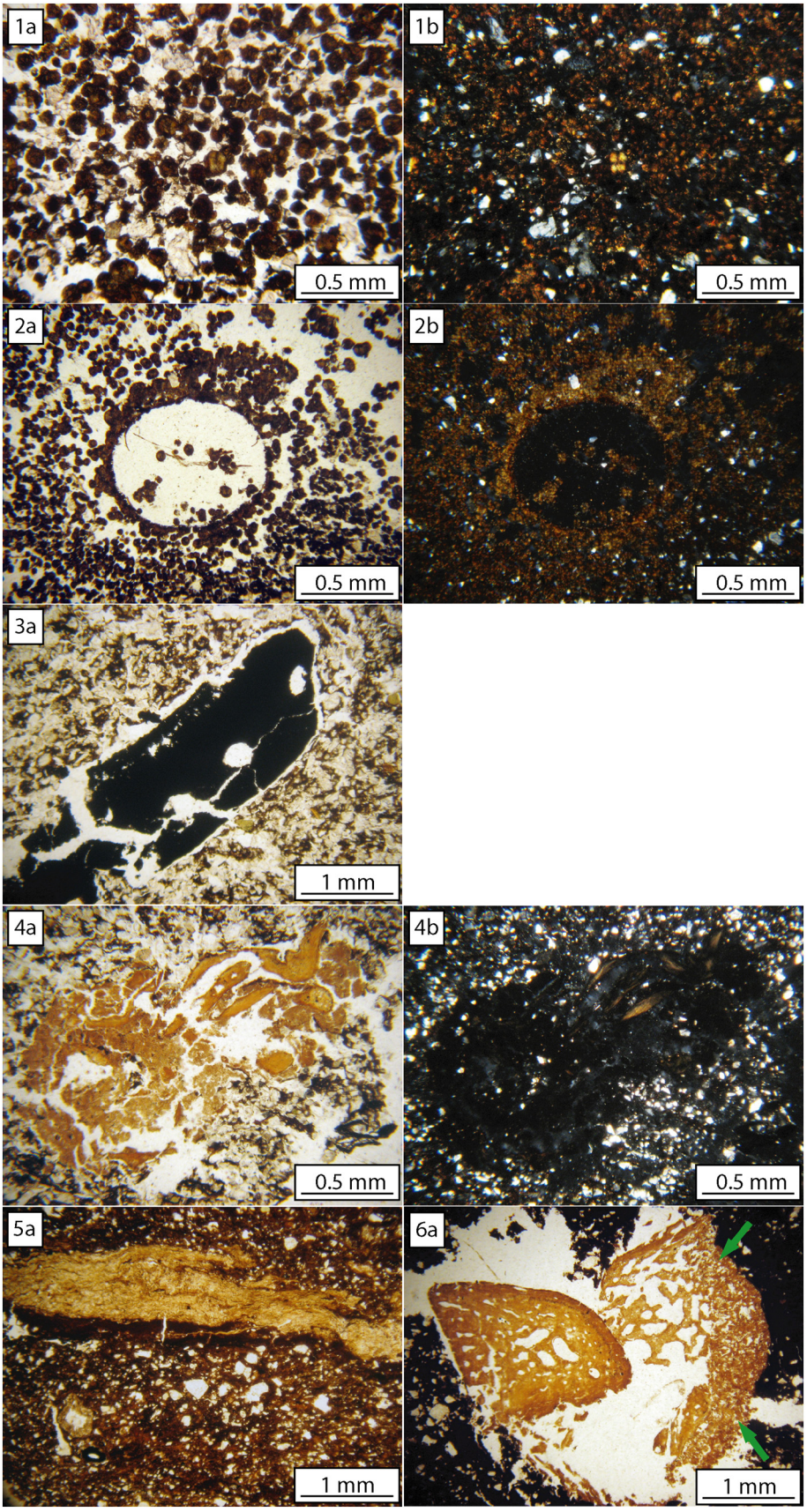

Fig. 4. Micromorphological thin-sections from unit VII (1, 2, 3, 5) and IX (4, 6). Photos a: plane polarized light (PPL) Photos b: crossed pollard light (XPL).

OM (mean 8.6%) and few $CaCO_3$ (0.7%), except for T1 (5.0%). The mean amount of sand situates around 45%. The grain-size is very similar to the underlying sediment, however it is generally more clayey. Closest to the palaeochannel this unit contains high amounts of OM (up to 18%), whereas $CaCO_3$ increases at the levels with iron-manganese concretions. Unit V is interpreted as the result of pedogenesis during a phase of low local water level.

Unit VII: organic silt forming a relatively homogeneous layer of maximum c. 40 cm thickness, only occurring at the contact between the levee and the palaeochannel. The sediment consists of blackish to greyish, slightly sandy silt with rather diffuse boundaries.

According to the analyses, this unit can be classified as poorly sorted, very fine sandy coarse silt, presenting an important variability. The clay content is higher in the lower levels, while the sand content increases towards the upper parts of the levee and from the base to the top of the unit. Within T3 the mean values are 40% sand, 57.6% silt and 2.4% clay. $CaCO_3$ amounts to <1%, OM has a mean value of 9%. The genesis of this unit is discussed in detail below.

Unit IX: silty peat with a maximum thickness of 2.6 m covering units V (T1) and VII (T3). This brown to blackish peat is strongly mixed with plant remains and vivianite. The darker levels result from more intense degradation of plant material. At its base the peat is much more sandy, locally forming beige layers of up to 10 cm thickness. Locally peat occurs interstratified with the underlying unit VII.

The OM content gradually increases from 27.1% at the base to a maximum of 79% higher-up, while the amount of $CaCO_3$ remains constantly very low (mean 1.4%). The grain-size is very variable, reaching gravel but dominated by silt. The coarser fraction is classified as slightly very fine gravelly, very coarse silty fine sand and very coarse silty very fine sand. Peculiar is the drop of clay below 1% in T3. This peat unit formed in a swamp that gradually spread over the entire valley floor under influence of a rising groundwater level. The swamp was occasionally flooded.

3.2. Micromorphology (Fig. 4)

Unit VII: The mineral fraction consists of well-sorted, very fine and fine sands. These are surrounded by fine, dark brown and blackish (PPL) organic material of vegetal origin. The lower limit of this unit is abrupt (Fig. 4-1a, b). Porosity is absent. Higher up we can observe cm-vide areas which underwent extrusive growth of siderite ($FeCO_3$) crystals with spherulitic morphology (Fig. 4-2a, b). Siderite appears to be concentrated along a c. 5 cm-thick band in the middle part of this unit. Siderite is reported to form under strongly reducing conditions (Lindbo et al., 2010, p. 141) and is found in bog ores of the Belgian Campine in association to root pseudomorphs like in the sample analysed here (Stoops, 1983, p. 179, 185).

The environment of deposition is characterized by a progressive increase of the energy of the sedimentary environment. Moving towards the top, in fact, we observe a higher overall content of sand (up to 55–60% vs 30% in the lower part) and a coarser grain size (i.e., more fine sand than silt and very fine sand). We also observe an increase in the porosity (mostly vughs), which might suggest a period, even just a season, of temporary lower sedimentation rate and sub-aerial exposure. In the same thin-section there is also an increase in the amount and size of plant material fragments, with some sub-millimetric fragments of wood. In the topmost part of this thin section we begin to observe some coarse charcoal fragments, among which one burnt nut or fruit pericarp (Fig. 4-3a) and, interestingly, a carnivore-omnivore coprolite containing bone fragments (Fig. 4-5a). The tendency to increase in grain-size disappears in the topmost centimeters, where the sand content decreases slightly.

Unit IX: is initially made up by laminated organic muds (Fig. 4-4a, b) in which silt and very fine sands are dispersed. These organic muds grade towards the top of the unit to peat-like material, with a lower amount of mineral grains. We therefore see a rather abrupt passage from a dynamic environment in VII to a lower-energy setting in unit IX. Moreover, the deposition becomes more 'terrigenous' to the top, with the formation of peat-like materials as the channel was gradually infilled. In a thin section there is one fragment of bone (Fig. 4-6a), which appears severely weathered and partially dissolved, with neoformations of manganese. Bone weathering is probably the result of pH conditions unfavorable for bone preservation, as when pH is below 8, bioapatite begins to be altered and microbial attack takes place (Villagran et al., 2017).

3.3. Pollen, NPP and microcharcoal

The preservation of palynomorphs in unit VII is poor (average score 2), while in the peat (unit IX) it is moderate to poor (average score 2.5). Five local biozones, some with subzones, have been defined at the site, of which K2 (a and b) and K3a are present in the sections presented in this paper (Fig. 5).

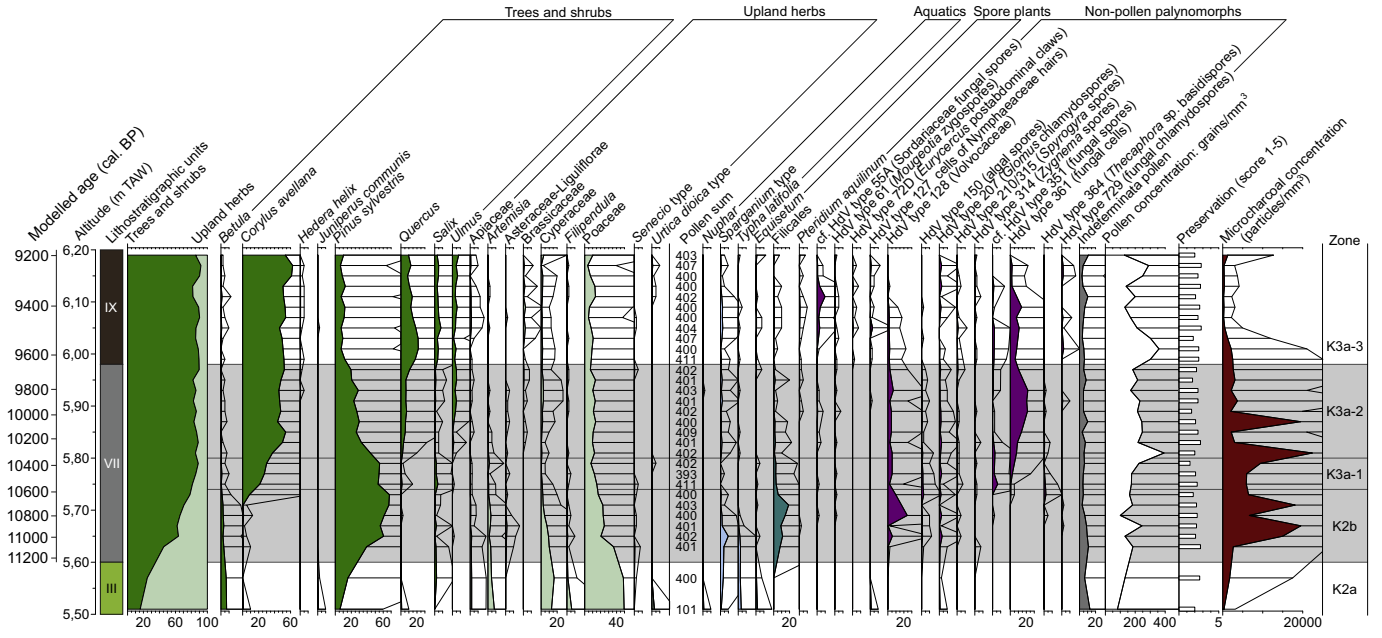

Fig. 5. Pollen percentage diagram (selected taxa) of the analysed sequence in T3. Full counts in supplementary data Table 2. Ages have been modelled according to the age-depth model of Blaauw (2010), based on the selected dates of the Bayesian analysis.

3.3.1. Zone K2a (5.50–5.60 m TAW): NAP dominant

This biozone corresponds to lithological unit III. The regional vegetation is characterized not only by high NAP percentages, but also by a high taxonomic diversity of herbs, including Poaceae (c. 50%), Cyperaceae, *Artemisia*, *Filipendula* and low amounts of many other herb taxa (not all depicted in Fig. 5). By contrast, the AP is much less diverse with c. 7% *Betula*, and low values of *Pinus*, *Salix* and *Juniperus*. These spectra point to grassland and open birch forest, while pine was not yet part of the vegetation. This may correspond to the Lateglacial or Preboreal vegetation in the region (Verbruggen et al., 1996; Storme et al., 2017). Radiocarbon dates from T1 confirm an Early Holocene age. Small amounts of aquatics and algae indicate a local predominantly lacustrine environment, while some reworked microfossils indicate phases of fluvial input. The microcharcoal concentration increases towards the top of the zone, from a few hundred to c. 1700 fragments per mm^3.

3.3.2. Zone K2b (5.60–5.74 m TAW): Pinus dominant

This biozone corresponds to the basal part of unit VII. The regional vegetation is characterized by high values of *Pinus*, up to c. 70%, while NAP show a decreasing trend. Filicales exceed 10% in this zone. The vegetation was dominated by pine forests, as is common in the later part of the Preboreal in the Scheldt Basin (Verbruggen et al., 1996; Storme et al., 2017). The marked occurrence of Filicales can point to an undergrowth of ferns in the pine forest or to marsh ferns (*Thelypteris palustris*) growing in the palaeochannel itself, as deduced for several other sites from the Scheldt valley (Storme et al., 2017). On a local level pollen of *Sparganium* and *Typha latifolia* in the lower part of the zone and several types of algal remains point to shallow wet conditions. Fungal spores are mostly absent, except for *Glomus*, the latter indicating input of eroded and transported material. The microcharcoal concentration is high in the entire zone and reaches almost 20,000 particles per mm^3 at two levels.

3.3.3. Zone K3a (5.74–6.22 m TAW): presence of Corylus (>5%), Quercus and Ulmus

This biozone includes the upper part of unit VII and the base of unit IX. The arrival of *Corylus*, *Quercus* and *Ulmus* marks the start of this zone, which is part of the Boreal biozone in the Scheldt basin (Verbruggen et al., 1996; Storme et al., 2017). The NAP is of minor importance in the entire zone, with Poaceae as dominant taxon.

Within this biozone, the relative abundances of the tree taxa fluctuate and allow to delimit three subzones:

K3a-1: 5.74–5.80 m TAW: *Pinus* remains high (c. 55%), while *Corylus* rises to c. 30%. *Salix* and Filicales are both present with c. 3%.

K3a-2: 5.80–5.98 m TAW: *Corylus* is stable at c. 50%. *Quercus* and *Ulmus* appear with low percentages (respectively c. 6% and 4%). *Pinus* decreases in the base and reaches c. 25%. *Hedera helix* appears in the top of this subzone.

K3a-3: 5.98–6.06 m TAW: *Corylus* and *Ulmus* remain stable, while *Quercus* (c. 20%) and *Salix* (c. 5%) show a peak. *Pinus* is no longer locally present (< 10%). This subzone corresponds with the base of the peat (unit IX).

These pollen spectra reflect the transition from a mixed forest to a deciduous forest as is typical for the region due to postglacial migration of trees in NW Europe (Verbruggen et al., 1996; Storme et al., 2017). The high temporal resolution of this diagram reveals that the expansion of *Corylus*, *Ulmus* and *Quercus* did not take place exactly at the same time, but happened in successive phases.

On the local level *Sparganium* and algal remains (HdV type 61, 128, 150 and 210) are present in low amounts throughout the zone. This points to a moist environment without permanent subaqueous conditions at the sampled location. Various types of fungal spores occur, of which HdV type 361 reaches up to c. 20% in the middle of the zone. These grew on decaying plant material and possibly also on animal dung. *Glomus* is continuously present in the base (unit VII, c. 2%), which points to a limited input of reworked material.

In the first subzone (K3a-1), microcharcoal concentrations remain very high (5000 to 10,000 fragments/mm^3). The second subzone (K3a-2) shows a baseline of c. 2500 fragments/mm^3, with two peaks of c. 20,000 fragments/mm^3. In the top (K3a-3), the concentrations decrease from c. 2500 to <500 fragments/mm^3.

3.4. Plant macroremains

The preservation of the waterlogged and charred macroremains clearly increases from the base (unit VII) to the upper parts (unit IX) of the sequence (Fig. 6). In the lowermost half of unit VII they are almost completely absent. The few specimens in the uppermost half mainly belong to nitrophilous taxa (*Sambucus*). Near the top of unit VII, we notice some specimen of *Mentha* cf. *aquatica* and *Lemna* sp. In unit IX, the total number of waterlogged macroremains increases as well as the number of herbs types. *Sambucus* on the other hand becomes less frequent. Among the charred remains there is a predominance of hazelnut shell fragments.

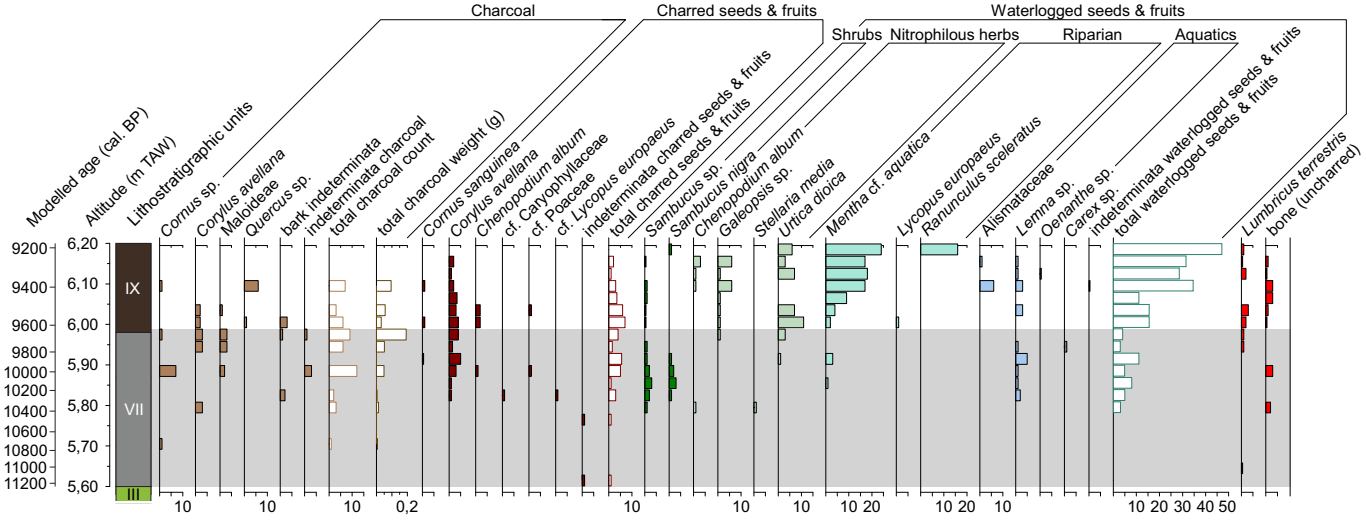

Fig. 6. Macroscopic charcoal, charred and waterlogged seeds and fruits within T3.

3.5. Macroscopic charcoal

Nine out of the twenty studied samples yielded charcoal fragments >2 mm (Fig. 6). In the lowermost three samples of unit VII no charcoal has been found but the residues of these samples contained a large number of iron concretions that are likely to have been formed around the organic material originally present in the sediment, and thus potentially obscuring or destroying macroscopic charcoal. The upper half of unit VII and lower levels of unit IX yielded very small quantities of macroscopic charcoal. The studied charcoal fragments originate from at least four different taxa, i.e. *Cornus* sp., *Corylus avellana*, Maloideae (Rosaceae subfamily which includes *Malus*, *Pyrus*, *Crataegus* and *Sorbus*) and *Quercus* sp.

3.6. Archaeological finds

Spatial analysis of the sieved prehistoric remains from the levee top revealed the presence of at least 13 clusters, called artefact loci (Fig. 7). These probably represent Mesolithic dwelling-spaces, in which various domestic activities were performed, such as lithic tool production, hide scraping, plant processing and bone working among others (Vandendriessche et al., in press). Most of these activities were conducted in the vicinity of open surface-hearths, preserved as small accumulations of overheated artefacts (Fig. 7) and burnt ecofacts, in particular charred hazelnut shells and calcined animal bone (Sergant et al., 2006). The total absence of charcoal in these features is most likely due to weathering (rain, frost, wind), as charcoal is more fragile than bone and nut shell.

Spatial analysis yielded evidence of possible post-depositional disturbance of the Mesolithic settlement remains. First it could be observed that the boundaries of some lithic loci, especially C10 (Fig. 7), are much less sharp and more diffuse along the steep southern slope of the levee, suggesting downslope post-depositional movement of at least part of the assemblage. Secondly, artefact refitting in T3 seems to corroborate this fact. Out of the total of 485 lithic artefacts in this zone, 86 could be refitted. Up to 70% of the resulting refit lines (n = 56) are oriented in the general direction of the slope (at an angle between 90 and 180°) with a clear peak in SE direction (Fig. 8). Although it seems unlikely that this disproportionate amount of artefact movements along the slope could be the consequence of anthropogenic actions, further refitting will be necessary to assess the spatial integrity of the other loci and to provide comparative data for the T3 test-case.

3.7. Chronological analysis

3.7.1. Palaeoenvironmental dating results

The master sequence T3 yielded 19 radiocarbon dates, spread over units VII (11 dates) and the lower half of IX (8 dates). It was decided to eliminate the dates on charred hazelnut shells (n = 3) from the Bayesian modelling as these most likely represent anthropogenic samples, i.e. settlement waste from hearths dumped and/or washed down from the levee top. Bayesian modelling finally resulted in the elimination of an extra 5 dates from macroremains because of an Agreement Index below 60% (Table 1). After elimination a final model with an Agreement Index of c. 84% was obtained, which makes the model highly reliable (Fig. 9).

The modelled results (Table 2; Fig. 9) indicate that the deposition of the slope sediments in T3 started between c. 11,810–11,180 cal BP

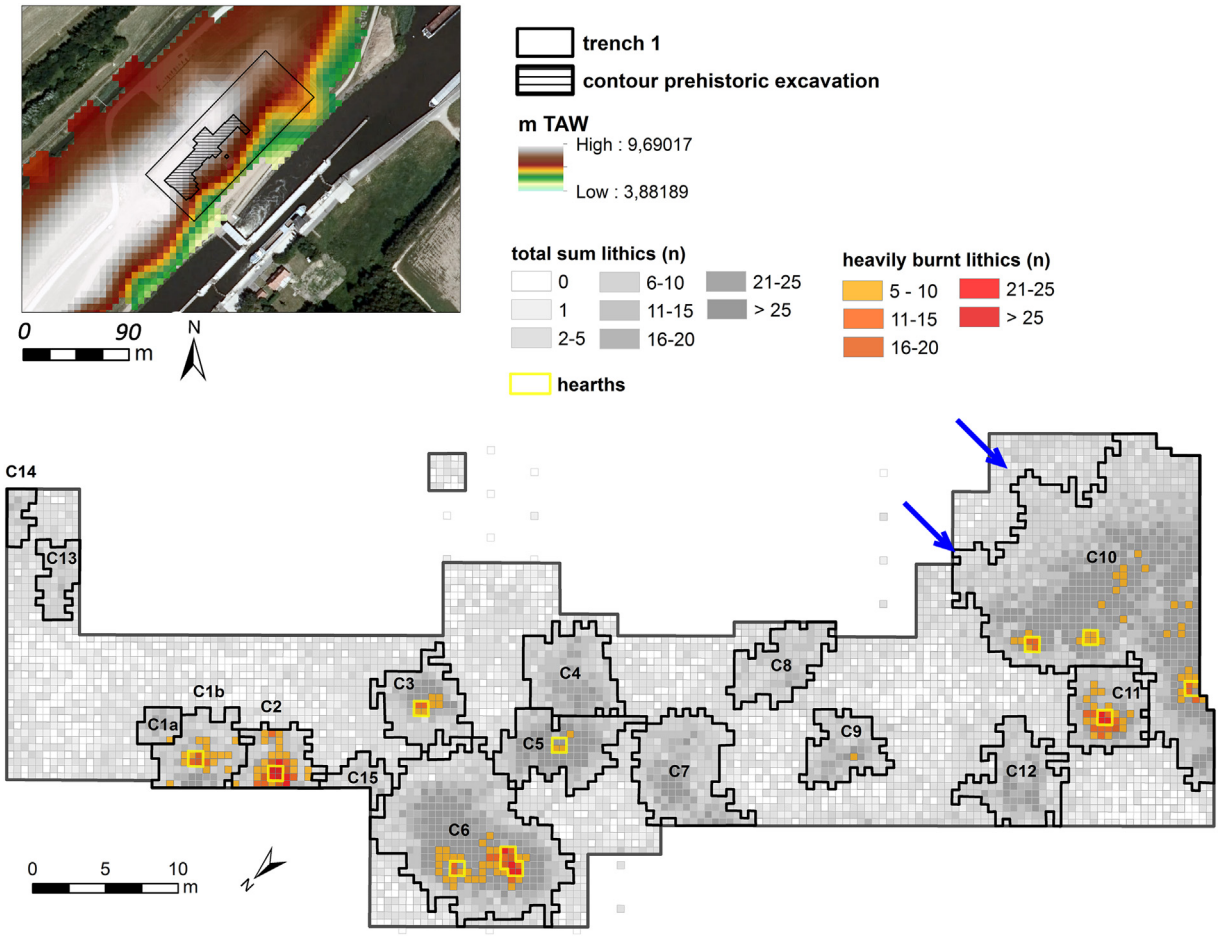

Fig. 7. Distribution plan of the Mesolithic artefacts density with indication of the limits of individual loci and surface-hearths. The blue arrows indicate the loci with diffuse boundaries.

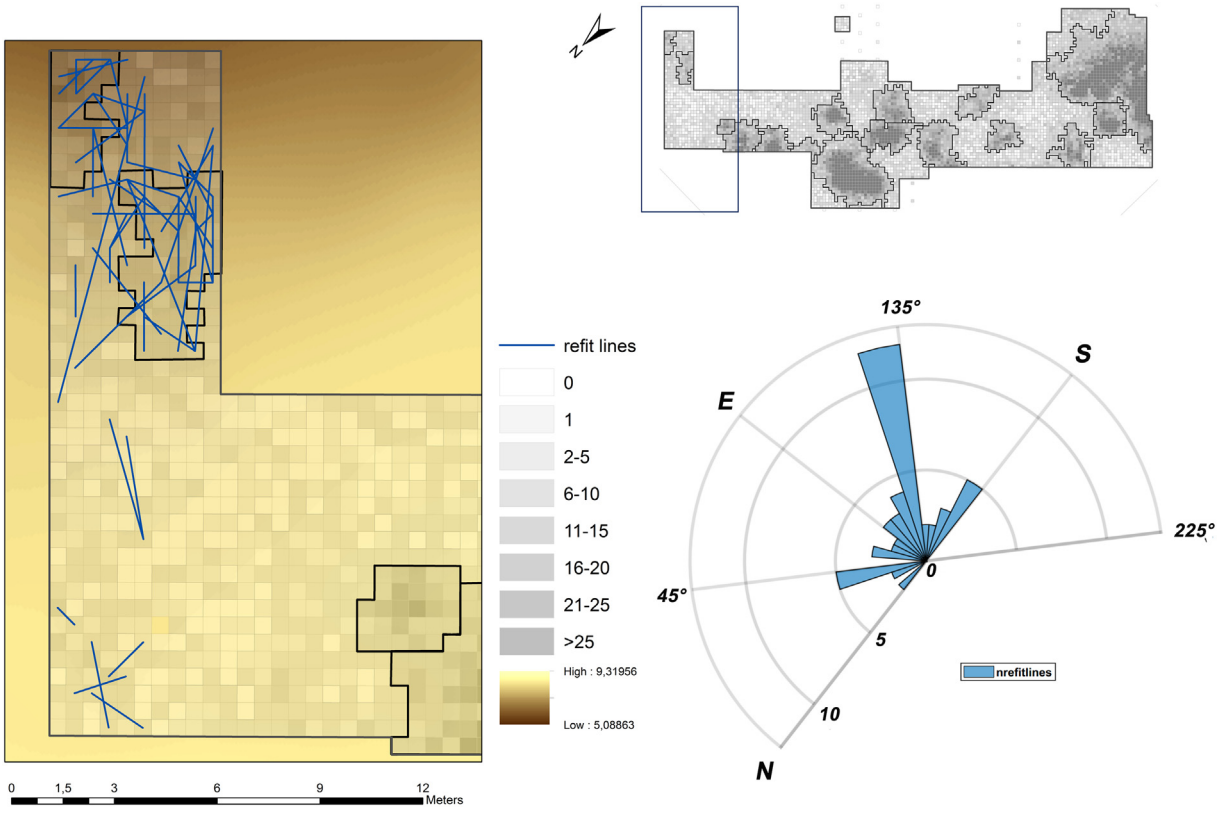

Fig. 8. Distribution map of the refitted lithic artefacts in T3 (left) and a graph presenting the orientation of refitted artefacts (right).

(95.4% probability), and most likely between c. 11,390–11,195 cal BP (68.2% probability). According to the model slope sedimentation ended between c. 9880–9610 cal BP (95.4% probability), most likely between c. 9850–9700 cal BP (68.2% probability). This timing is also corroborated by a single radiocarbon date in T1 (RICH-24264: 8996 ± 39 uncal BP), which is situated between c. 10,240–9940 cal BP (95.4%

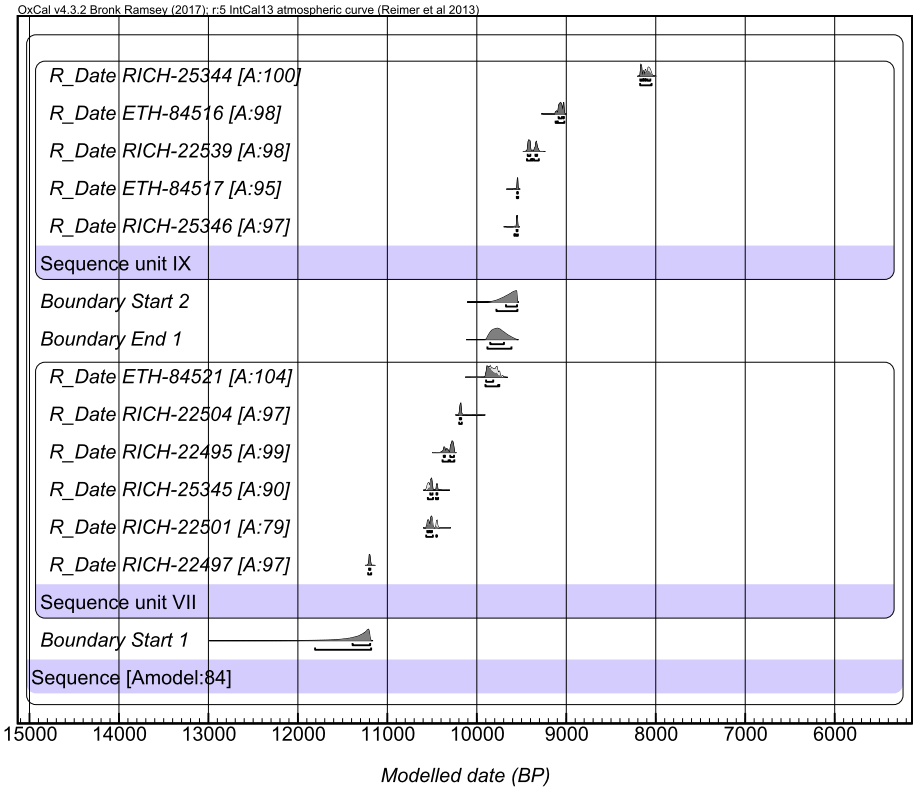

Fig. 9. Bayesian model of the radiocarbon dates from T3.

probability), and most probably between c. 10,230–10,175 cal BP (68.2% probability).

However, it can be assumed that the model just provides a minimum estimation. Two dated samples of animal bone (Table 1) from unit VII in T3 (RICH-22499: 8304 ± 40 uncal BP) and T1 (RICH-24211: 8383 ± 39 uncal BP) give a calibrated age between resp. c. 9440–9140 cal BP and c. 9490–9325 cal BP (95.4% probability) or between resp. c. 9410–9275 cal BP and c. 9490–9300 cal BP (68.2% probability). These dates on archaeological samples from within unit VII might indicate that the deposition continued until 9400/9300 cal BP, perhaps locally. Alternatively, a sedimentological hiatus between the end of the slope deposition and start of peat growth needs to be considered. In that case the archaeological samples indicate waste dumping by Mesolithic hunter-gatherers on top of the slope sediments. The latter is supported by the larger dimensions of the bone remains at this level compared to the lower levels of unit VII.

3.7.2. Archaeological dating results

Based on several morpho- and technological features of the lithic artefacts, mainly the armatures, the hunter-gatherer occupation on the levee top can be dated to the archaeological stages of the Early and Middle Mesolithic (Vandendriessche et al., in press). Some dispersed trapezes also point to human presence during the Late Mesolithic, but given the lack of associated knapping waste, its nature is clearly different compared to the earlier phases (i.e. hunting episodes rather than settling).

Bayesian statistical "Phase" analysis of the available radiocarbon dates on burnt hazelnut shells (Model Agreement c. 91%) indicates a start of the Early Mesolithic occupation between c. 10,740 and 10,430 cal BP (95.4% probability), and most likely between c. 10,630 and 10,490 cal BP (68.2% probability) (Table 2; Fig. 10). The end situates between c. 9845 and 9415 cal BP (95.4% probability) or between c. 9685 and 9530 cal BP (68.2% probability). Lack of datable material within the Middle Mesolithic loci does not allow to determine the chronology of the later occupation. Yet, it has been defined in earlier studies (Robinson et al., 2013; Crombé, 2018) that the Middle Mesolithic in the southern North sea basin encompasses the period of c. 9350 to 8350 cal BP. Not knowing the exact duration of the Middle Mesolithic occupation at Kerkhove, the date of c. 9350 cal BP can thus be used as *terminus post quem*.

Finally, the single successful radiocarbon date on animal bone from the levee top should be mentioned (Table 3). Spatially not associated with a specific artefact locus (so-called off-site find) this date is clearly younger than the bulk of hazelnut dates as it refers to the period of c. 7250–7010 cal BP (95.4% probability). Most probably it connects with Late Mesolithic hunting activities on the site.

4. Discussion

Based on the results of the different analyses the organic silty deposit VII at the foot of the levee at Kerkhove can be interpreted as a slope deposit. There is an overlap in grain size with the palaeosol (unit V) developed on the Lateglacial levee top (unit II). The finer grain-size of layer VII probably points to a sorting during transport of this soil material. In addition, there is the gradual decrease in thickness of the deposit from the slope's foot towards the river channel, excluding an alluvial nature. The latter is also supported by the marked sedimentological differences with the underlying unit III, interpreted as a lacustrine/alluvial deposit, which is characterized by a much higher $CaCO_3$ and a much lower OM content. Furthermore there is the presence of spores of *Glomus*, an arbuscular mycorrhizal fungus that is often associated with redeposited material from eroded soils (van Geel et al., 1989; Silva-Sanchez et al., 2014; Garrett et al., 2018). However, in this case the spores may also originate from fungi living on roots of the peat-forming vegetation that developed on top of unit VII (Kolaczek et al., 2013). Finally, there is spatial evidence (e.g. refittings) which indicates that part of the lithic artefacts (and probably also the animal bones and carbonized plant macroremains) found in unit VII originates from occupation levels on the top of the levee and was washed down towards the levee base.

Precisely which geomorphic process was responsible for the observed hillslope erosion currently remains unclear. Yet, the slope appears to be too gentle to consider mass wasting like soil creep. In any case, no sedimentary structures of this process have been observed during the extensive archaeological dig of the levee. The same applies to rilling, gullying or piping structures. On the other hand bioturbation might have blurred these traces, although it is difficult to believe the latter were all erased. The low sedimentation rate of unit VII rather implies a slow and repeated erosional process, such as raindrop impact or water runoff (Selby, 1993). Detachment by raindrop impact just needs a soil exposed to the force of drops whereas runoff is generally limited to a small portion of the area.

The modelled radiocarbon evidence allows to date the start of the deposition of this slope sediment around c. 11,400/11,200 cal BP, which corresponds to the late Preboreal, a date also corroborated by the pollen data. The base of unit VII belongs to biozone K2b characterized by a predominance of *Pinus* and an absence of *Corylus* which is indicative of the *Pinus* stage of the late Preboreal in the Scheldt basin and beyond (zone 5 in the Netherlands, Hoek, 1997; SB 3 in the Scheldt basin, Storme et al., 2017). The exact duration of the erosion is more difficult to determine. In transect 3 clastic deposition ended around c. 9850–9700 cal BP and was replaced by peat accumulation due to wetter conditions at that location. However, there may have been a sedimentological hiatus between both, during which the top of the slope deposit formed a dry surface on which Mesolithic hunters dumped bone waste material. In short, the formation of unit VII as a result of slope instability lasted for about 1500 years, from the late Preboreal till the middle of the Boreal.

Sediment erosion is only possible when the soil surface is unprotected. However, this does not necessarily imply a total lack of vegetation, as there is plenty of evidence of slope erosion in forested areas (Selby, 1993). An essential precondition, however, is the absence or advanced deterioration of the undergrowth vegetation, e.g. grasses and shrubs. In the case of Kerkhove this implies that vegetation on (parts of) the levee top and/or slope must have been deteriorated over a considerable time, whether or not continuously. An important question relates to the possible trigger(s) of reduced vegetation during this long period of time. In other European regions Early Holocene soil erosion either by wind or surface water has been linked to natural (wildfires, wind-throws, animal trampling and browsing (Dreibrodt et al., 2010a, 2010b)) or anthropogenic factors (trampling, controlled forest burning (Sevink et al., 2018)) or a combination of both (Tolksdorf and Kaiser, 2012; Tolksdorf et al., 2013). The fact that slope instability at Kerkhove already started before the onset of the human occupation on the levee top and ended earlier (Fig. 11), strongly suggests that the activities of the local hunter-gatherers, such as trampling and controlled burning, cannot be the principal responsible. According to the Bayesian model, occupation did not start before c. 10,600/10,500 cal BP, which is more than half of a millennium later than the beginning of slope erosion. By that time the slope deposit had already reached almost half of its total thickness. In addition, there is no firm proof of human presence in the Early Holocene, prior to 10,700 cal BP, in the entire Scheldt basin (Crombé et al., 2009), making it very unlikely that slope erosion is due to human activities at all. Moreover, on-site human occupation lasted until at least c. 9350 cal BP which is several centuries later than the end of the slope erosion (Fig. 11). All these arguments make it more likely that slope instability was initiated by natural processes rather than by human land use.

In this context the vertical distribution of the microcharcoal is very informative. Clearly the overall distribution of microcharcoal correlates with the thickness of unit VII (Fig. 11). Microcharcoal frequency is continuously high (minimum c. 2000 particles per mm^3), reaching major peaks of c. 20,000 particles per mm^3 at four different levels, indicating repeated events of intensive forest fires during the entire length of

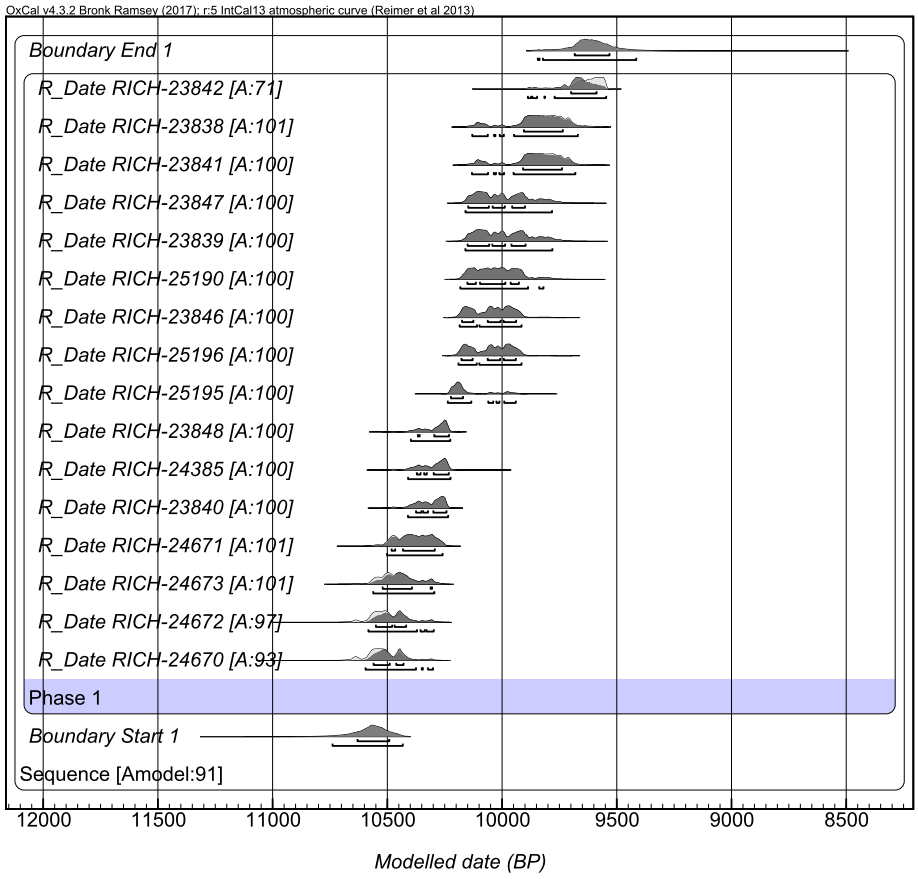

Fig. 10. Bayesian model of the human occupation.

formation of the slope deposit. Once peat started to grow on top of the slope deposits, the concentration of microcharcoal decreased considerably from c. 2500 to <500 fragments/mm^3. Due to the preparation technique it is however not possible to determine whether the microcharcoal originates from local and/or regional fires. Yet, the absence of macrocharcoal in the lowest half of unit VII might suggest that initially it concerned regional fires. If so, forest fires cannot be held responsible for the slope erosion of the levee at Kerkhove. However, it cannot be excluded that the vertical distribution of macrocharcoal, as well as the other plant macroremains, is biased to a certain degree as a result of taphonomic factors: oxidation processes probably affected the preservation of the botanical remains as there are indications that the slope deposit has been subject to temporal sub-aerial exposure (cf. 3.2; 3.3). The presence of iron concretions in the lowest three sampled levels confirms the occurrence of such oxidizing conditions. Alternatively, it must be envisaged that the colluvial material derived from a very narrow steep zone at the foot of the levee, where only annual, fibrous plants could develop as a result of seasonally fluctuating water levels. In that case no ligneous plants would have been present in the source area of the colluvium and fires would not produce charcoal in that area. However, it is not certain that this zone would have been broad enough to account for the volume of the colluvial layer. Finally, the type of forest fire may also be responsible for the lack of macrocharcoal. It is well possible that the levee was affected by surface fires rather than crown fires (Moore, 2000). Indeed, the former only affect vegetation fuel at or near the ground, such as surface litter and undergrowth vegetation. According to a study by Heinselman (1981) light surface fires with a return interval of 1 to >25 years are the most frequent types of fires within the fire cycle of a forest.

In contrast macrocharcoal and carbonized macroremains, such as hazelnut shells, are well represented in the upper half of the slope deposit (Fig. 11). They appear from c. 5.80 m TAW onwards (c. 10,400/10,350 cal BP) and gradually increase into the lower levels of the peat. However, it is doubtful whether these burnt botanical remains can be linked with local forest fires, since there is no clear stratigraphical correlation with the microcharcoal, except for level 5.89 m TAW. On the contrary, most macrocharcoal fragments are situated at the transition from unit VII to IX, where microcharcoal frequency is already lower. In fact, the appearance of burnt plant remains is more or less synchronous with the start of the human occupation of the levee top, which reinforces the hypothesis that they most likely are not related to local forest fires, but rather to human activity such as the burning of hearths. The latter have been found, often in association with considerable numbers of charred hazelnut shells and animal bones, within several concentrations of settlement waste on the levee top, testifying of the intensive use of hearths by the occupants of the site for cooking, warming and other domestic activities.

Other possible triggers for reduced vegetation during the slope erosion are series of windthrows, animal trampling and/or climatic changes, but there is currently little supporting evidence for these processes at Kerkhove. The timing of the slope erosion does not match with any known climatic fluctuation, which might have affected the vegetation to such a degree that it resulted in bare surfaces. In other European regions (Dreibrodt et al., 2010a; Hoffmann et al., 2008; Lucke et al., 2003) a correlation has been demonstrated with one or several short but abrupt cooling events, such as the 10.3, 9.3 and 8.2 ka cal BP events, as identified in several deep sea (Bond et al., 1997) and Greenland ice core records (Rasmussen et al., 2007). It is argued that increased coldness and dryness during these 100 to 150 years lasting periods affected the existing stands of pine forests, creating large quantities of very flammable litter. Lightning would have led to extensive wildfires, which triggered slope erosion on steep hill flanks. Although slope deposition at Kerkhove chronologically does not match with any of these cooling events the dominance of pine forests might

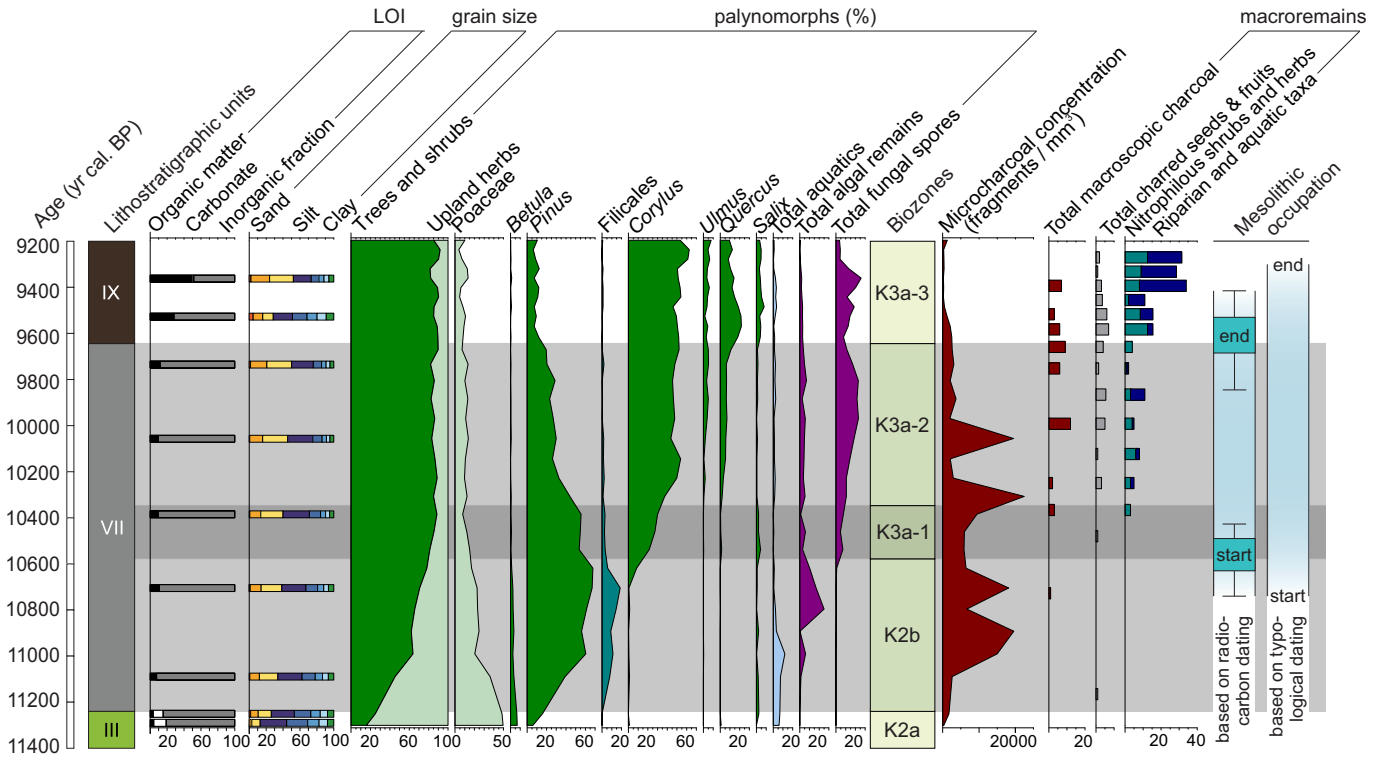

Fig. 11. Multi-proxy diagram combining evidence from sedimentological analyses, pollen, charcoal and plant macroremains against the chronology of the human occupation of the levee.

also have been the main trigger for the forest fires. From the multi-proxy Fig. 11 it is clear that slope erosion took place during the period in which pines dominated the environment. Once pines were replaced by oak both slope erosion and forest fires came to an abrupt halt. This might be considered as an extra argument for a purely natural origin of the forest fires (and thus slope erosion), as it is well-known that deciduous forests are much less vulnerable to burning than coniferous forests (Rowe and Scotter, 1973; Zolitschka, 1992; Dreibrodt et al., 2010b; Bishop et al., 2015; Marlon et al., 2013; Cui et al., 2015). It thus seems that there is a very close correlation between pine forests, wildfires, and slope instability during the late Preboreal and Boreal.

In short, although direct evidence for local forest fires affecting the vegetation on the levee is currently lacking, other natural mechanisms or an anthropogenic origin of the slope erosion is very unlikely.

5. Conclusions

Early Holocene slope erosion by surface runoff is already well-attested in hilly regions with pronounced topography such as Central Europe. The site of Kerkhove demonstrates that similar processes were also active in regions with more subtle topographical gradients and smaller features such as a levee, proving that lowland areas are also affected by pre-agriculture slope erosion. In addition the existence of similar, though less documented sites in the Scheldt basin, such as Valenciennes (Boulen et al., 2014) and Rebecq (Fechner et al., 2014), might indicate that the impact of Early Holocene slope erosion is much more general than presumed.

Concerning the triggers, the site of Kerkhove yielded convincing evidence for a natural rather than an anthropogenic origin of erosion. The hillslope sedimentary dynamic fits in the geomorphic system of the Early Holocene which was in a transient state (Hoffmann, 2015). Compared with the present day, soils back then would be more fragile as they contained little organic matter and the structure was not yet fully developed. Despite the absence of macrocharcoal fragments, it is concluded that slope erosion was most likely induced by repeated and intensive surface wildfires in pine forests. As the latter covered large parts of NW Europe, especially during the late Preboreal and Boreal and locally even longer (e.g. sandy lowlands), it can be expected that pre-agricultural slope erosion was much more wide-spread than hitherto assumed. In order to assess its full impact future geomorphological research should therefore focus more on precise dating of colluvial deposits, rather than assuming that this type of sedimentation just started with the appearance of the first farming communities in the Neolithic.

In addition this study has demonstrated that wildfires and slope erosion apparently did not prevent or discourage contemporaneous hunter-gatherers to seasonally settle on the affected levee. Perhaps they actually were attracted by the forest openings created by the wildfires, because of the presence of young and fresh undergrowth vegetation among which edible plants and fruit- and nut-bearing shrubs (e.g. wild apple, hazel, blackberry and elder), but also various herbaceous plant species (e.g. nettle, rush, …) which could be used for the production of basketry, nets, etc. The latter is corroborated by the discovery of microscopic use-wear traces on several stone tools, resulting from the processing (splitting and scraping) of siliceous plants. Furthermore, the natural opening on the levee was probably also very suited for erecting a camp-site; it provided an easy and direct access to the nearby river for fishing, hunting and gathering plants as the wildfires had burnt down all obstructing vegetation.

Supplementary data to this article can be found online at https://doi.org/10.1016/j.geomorph.2019.03.025.

Acknowledgements

The multidisciplinary excavation and analysis of the wetland site of Kerkhove was entirely financed by the “Vlaamse Waterweg nv” and the European Union, Trans-European Transport Network (TENT-T). We are very grateful towards project manager ir. Sandrien Paeleman.

References

Bakker, M., Van Smeerdijk, D.G., 1982. A palaeoecological study of a late holocene section from “Het Ilperveld”, western Netherlands. Rev. Palaeobot. Palynol. 36, 95–163.

Beug, H.-J., 2004. Leitfaden der Pollenbestimmung fur Mitteleuropa und angrenzende Gebiete. Verlag Friedrich Pfeil, München.
Bishop, R.R., Church, M.J., Rowley-Conwy, P.A., 2015. Firewood, food and human niche construction: the potential role of Mesolithic hunter-gatherers in actively structuring Scotland's Woodlands. Quat. Sci. Rev. 108, 51–75.
Blaauw, M., 2010. Methods and code for 'classical' age-modelling of radiocarbon sequences. Quat. Geochronol. 5, 512–518 (Version 2.3.2).
Bond, G., Showers, W., Cheseby, M., Lotti, R., Almasi, P., deMenocal, P., Priore, P., Cullen, H., Hajdas, I., Bonani, G., 1997. A pervasive millennial-scale cycle in North Atlantic Holocene and glacial climates. Science 278, 1257–1266.
Boulen, M., Deschodt, L., Henton, A., 2014. Evolution morpho-sédimentaire et enregistrement pollinique atlantique dans le nord de la France: la séquence de Valenciennes "le vignoble" (vallée de l'Escaut, nord). Quaternaire 25 (4), 369–389.
Bronk Ramsey, C., 1995. Radiocarbon calibration and analysis of stratigraphy: the OxCal program. Radiocarbon 37 (2), 425–430.
Bronk Ramsey, C., 2009. Bayesian analysis of radiocarbon dates. Radiocarbon 51 (1), 337–360.
Cahen, D., Keeley, L.H., Van Noten, F.L., 1979. Stone tools, toolkits and human behaviour in prehistory. Curr. Anthropol. 20 (4), 661–683.
Cappers, R.T.J., Bekker, R.M., Jans, J.E.A., 2006. Digitale zadenatlas van Nederland. Barkhuis Publishing and Groningen University, Groningen.
Collcutt, S.N., Barton, R.N.E., Bergman, C.A., 1990. Refitting in context: a taphonomic case study from a Late Upper Palaeolithic site in sands on Hengistbury Head, Dorset (Great Britain). In: Cziesla, E., Eickhoff, S., Arts, N., Winter, D. (Eds.), The Big Puzzle, International Symposium on Refitting Stone Artefacts. Monrepos 1987. Studies in Modern Archaeology 1, Holos, Bonn, pp. 219–236.
Crombé, Ph., 2018. Abrupt cooling events during the Early Holocene and their potential impact on the environment and human behaviour along the southern North Sea basin (NW Europe). J. Quat. Sci. 33 (3), 353–367.
Crombé, Ph., Van Strydonck, M., Boudin, M., 2009. Towards a Refinement of the Absolute (Typo)chronology for the Early Mesolithic in the Coversand Area of Northern Belgium and the Southern Netherlands. In: Crombé, Ph., Van Strydonck, M., Sergant, J., Boudin, M., Bats, M. (Eds.), Chronology and Evolution within the Mesolithic of North-West Europe: Proceedings of the International Congress Chronology and Evolution in the Mesolithic of Northwest Europe (May 30th till June 1st 2007). Cambridge Scholar Publishing, Newcastle, pp. 95–112.
Crombé, Ph., Robinson, E., Boudin, M., Van Strydonck, M., 2013. Radiocarbon dating of Mesolithic open-air sites in the coversand area of the Northwest European Plain: problems and prospects. Archaeometry 55 (3), 545–562.
Cui, Q.Y., Gaillard, M.-J., Olsson, F., Greisman, A., Lemdahl, G., Zernova, G., 2015. A case study of the role of climate, humans, and ecological setting in Holocene fire history of northwestern Europe. Sci. China 58 (2), 195–210.
Dreibrodt, S., Lomax, J., Nelle, O., Lubos, C., Fischer, P., Mitusov, A., Reiss, St., Radtke, U., Nadeau, N., Meiert Grootes, P., Bork, H-R., 2010a. Are mid-latitude slopes sensitive to climatic oscillations? Implications from an Early Holocene sequence of slope deposits and buried soils from eastern Germany. Geomorphology 122(3–4), 351–369.
Dreibrodt, S., Lubos, C., Terhorst, B., Damm, B., Bork, H.-R., 2010b. Historical soil erosion by water in Germany: scales and archives, chronology, research perspectives. Quat. Int. 222, 80–95.
Fechner, K., Baes, R., Louwagie, G., Gebhardt, A., 2014. Relic Holocene colluvial and alluvial depositions in the basins of the Scheldt, the Meuse, the Somme, the Seine and the Rhine (Belgium, Luxemburg and Northern France). A prospective state of research in rescue excavations. The Archaeology of Erosion, the Erosion of Archaeology, pp. 147–190.
Folk, R.L., 1954. The distinction between grain size and mineral composition in sedimentary-rock nomenclature. J. Geol. 62, 344–359.
Folk, R.L., Ward, W.C., 1957. Brazos River bar: a study in the significance of grain size parameters. J. Sediment. Petrol. 27, 3–26.
Garrett, E., Fujiwara, O., Riedesel, S., Walstra, J., Deforce, K., Yokoyama, Y., Schmidt, S., Brückner, H., De Batist, M., Heyvaert, V., Team, QuakeRecNankai, 2018. Historical Nankai-Suruga megathrust earthquakes recorded by tsunami and terrestrial mass movement deposits on the Shirasuka coastal lowlands, Shizuoka Prefecture, Japan. The Holocene 28, 968–983.
Grimm, E.C., 2015. Tilia for Windows: Pollen Spreadsheet and Graphics Program. Version 2.0.41. Illinois State Museum, Research and Collections Centre, Springfield.
Hajdas, I., 2008. Radiocarbon dating and its applications. Quaternary studies. Q. Sci. J. 57, 2–24.
Heinselman, M.L., 1981. Fire intensity and frequency as factors in the distribution and structure of northern ecosystems. Fire Regimes and Ecosytem Properties: Proceedings of the Conference (USDA For serv, Washington, Gen. Tech. Rep WO-26).
Heiri, O., Lotter, A.F., Lemcke, G., 2001. Loss on ignition as a method for estimating organic and carbonate content in sediments: reproducibility and comparability of results. J. Paleolimnol. 25, 101–110.
Hoek, W.Z., 1997. Late-glacial and early Holocene climatic events and chronology of vegetation development in the Netherlands. Veg. Hist. Archaeobotany 6, 197–213.
Hoffman, J.L., 1992. Putting the pieces together: An introduction to refitting. In: Hofman, J.L., Enloe, J.G. (Eds.), Piecing Together the Past: Applications of Refitting Studies in Archaeology, British Archaeological Reports International Series 578, Oxford, pp. 1–20.
Hoffmann, T., 2015. Sediment residence time and connectivity in non-equilibrium and transient geomorphic systems. Earth Sci. Rev. 150, 609–627.
Hoffmann, T., Lang, A., Dikau, R., 2008. Holocene river activity: analysing ^{14}C-dated fluvial and colluvial sediments from Germany. Quat. Sci. Rev. 27, 2031–2040.
Kalis, A.J., Josef Merkt, J., Wunderlich, J., 2003. Environmental changes during the Holocene climatic optimum in central Europe - human impact and natural causes. Quat. Sci. Rev. 22, 33–79.
Kolaczek, P., Zubek, S., Blaszkowski, J., Mleczko, P., Margielewski, W., 2013. Erosion or plant succession — how to interpret the presence of arbuscular mycorrhizal fungi (Glomeromycota) spores in pollen profiles collected from mires. Rev. Palaeobot. Palynol. 189, 29–37.
Leroi-Gourhan, A., Brézillon, M., 1972. Fouilles de Pincevent: Essai d'analyse ethnographique d'un habitat Magdalénien. Gallia Préhistoire, VIIème supplement. CNRS, Paris.
Lindbo, D.L., Stolt, M.H., Vepraskas, M.J., 2010. Redoximorphic features. In: Stoops, G., Marcelino, V., Mees, F. (Eds.), Interpretation of Micromorphological Features of Soils and Regoliths. Elsevier, Amsterdam, pp. 129–147.
Lucke, A., Schlesera, G.H., Zolitschka, B., Negendank, J.F.W., 2003. A Lateglacial and Holocene organic carbon isotope record of lacustrine palaeoproductivity and climatic change derived from varved lake sediments of Lake Holzmaar, Germany. Quat. Sci. Rev. 22, 569–580.
Marlon, J.R., Bartlein, P.J., Daniau, A.-L., Harrison, S.P., Maezumi, S.Y., Power, M.J., Tinner, W., Vannière, B., 2013. Global biomass burning: a synthesis and review of Holocene paleofire records and their controls. Quat. Sci. Rev. 65, 5–25.
McGeehin, J., Burr, G.S., Jull, A.J.T., Reines, D., Gosse, J., Davis, P.T., Muhs, D., Southon, J.R., 2001. Stepped-combustion 14C dating of sediment: a comparison with established techniques. Radiocarbon 43 (2A), 255–261.
McGeehin, J., Burr, G.S., Hodgins, G., Bennett, S.J., Robbins, J.A., Morehead, N., Markewich, H., 2004. Stepped-combustion 14C dating of bomb carbon in lake sediment. Radiocarbon 46 (2), 893–900.
Moore, J., 2000. Forest Fire and Human Interaction in the Early Holocene Woodlands of Britain. Palaeogeogr. Palaeoclimatol. Palaeoecol. 164, 125–137.
Moore, P.D., Webb, J.A., Collinson, M.E., 1991. Pollen analysis. second edition. Blackwell, Oxford.
Mulitza, S., Prange, M., Stuut, J.B., Zabel, M., Von Dobeneck, T., Itambi, A.C., Nizou, J., Schulz, M., Wefer, G., 2008. Sahel megadroughts triggered by glacial slowdowns of Atlantic meridional overturning. Paleoceanography 23, 1–11.
Notebaert, B., Verstraeten, G., Vandenberghe, D., Marinova, E., Poesen, J., Govers, G., 2011. Changing hillslope and fluvial Holocene sediment dynamics in a Belgian loess catchment. J. Quat. Sci. 26 (1), 44–58.
Rasmussen, S.O., Vinther, B.M., Clausen, H.B., Andersen, K.K., 2007. Early Holocene climate oscillations recorded in three Greenland ice cores. Quat. Sci. Rev. 26, 1907–1914.
Reimer, P.J., Bard, E., Bayliss, A., Beck, J.W., Blackwell, P.G., Bronk Ramsey, C., Buck, C.E., Cheng, H., Edwards, R.L., Friedrich, M., Grootes, P.M., Guilderson, T.P., Haflidason, H., Hajdas, I., Hatté, C., Heaton, T.J., Hoffmann, D.L., Hogg, A.G., Hughen, K.A., Kaiser, K.F., Kromer, B., Manning, S.W., Niu, M., Reimer, R.W., Richards, D.A., Scott, E.M., Southon, J.R., Staff, R.A, Turney, C.S.M., van der Plicht, J., 2013. IntCal13 and Marine13 radiocarbon age calibration curves 0–50,000 years cal BP. Radiocarbon 55 (4), 1869–1887.
Robinson, E., Gelorini, V., Van Strydonck, M., Crombé, Ph., 2013. Radiocarbon chronology and the correlation of hunter-gatherer sociocultural change with abrupt palaeoclimate change: the Middle Mesolithic in the Rhine-Meuse-Scheldt area of Northwest Europe. J. Archaeol. Sci. 40, 755–763.
Rowe, J.S., Scotter, G.W., 1973. Fire in the Boreal forest. Quat. Res. 3, 444–464.
Ruff, M., Fahrni, S., Gaggeler, H.W., Hajdas, I., Suter, M., Synal, H.-A., Szidat, S., Wacker, L., 2010. On-line radiocarbon measurements of small samples using elemental analyzer and Micadas gas ion source. Radiocarbon 52 (4), 1645–1656.
Schoch, W., Heller, I., Schweingruber, F.H., Kienast, F., 2004. Wood anatomy of central European species. Online version. www.woodanatomy.ch.
Schweingruber, F.H., 1990. Microscopic Wood Anatomy, Structural Variability of Stems and Twigs in Recent and Subfossil Woods From Central Europe. EFWSL, Birmensdorf.
Selby, M.J., 1993. Hillslope Materials and Processes. Oxford University Press, Oxford.
Sergant, J., Crombé, Ph., Perdaen, Y., 2006. The 'invisible' hearths. A contribution to the discernment of Mesolithic non-structured surface hearths. J. Archaeol. Sci. 33, 999–1007.
Sevink, J., van Geel, B., Jansen, B., Wallinga, J., 2018. Early Holocene forest fires, drift sands, and Usselo-type paleosols in the Laarder Wasmeren area near Hilversum, the Netherlands: Implications for the history of sand landscapes and the potential role of Mesolithic land use. Catena 165, 286–298.
Silva-Sanchez, N., Martinez Cortizas, A., Lopez-Merino, L., 2014. Linking forest cover, soil erosion and mire hydrology to late-Holocene human activity and climate in NW Spain. The Holocene 24 (6), 714–725.
Stockmarr, J., 1971. Tablets with spores used in absolute pollen analysis. Pollen Spores 13, 615–621.
Stoops, G., 1983. SEM and light microscopic observations of minerals in bog ores of the Belgian Campine. Geoderma 30, 179–186.
Stoops, G., 2003. Guidelines for Analysis and Description of Soil and Regolith Thin Sections. Soil Science Society of America, Madison, WI.
Storme, A., Louwye, S., Crombé, P., Deforce, K., 2017. Postglacial evolution of vegetation and environment in the Scheldt Basin (northern Belgium). Veg. Hist. Archaeobotany 26, 293–311.
Tolksdorf, J.F., Kaiser, K., 2012. Holocene aeolian dynamics in the European sand-belt as indicated by geochronological data. Boreas 41, 408–421.
Tolksdorf, J.F., Klasen, N., Hilgers, A., 2013. The existence of open areas during the Mesolithic: evidence from Aeolian sediments in the Elbe-Jeetzel area, northern Germany. J. Archaeol. Sci. 40, 2813–2823.
van Geel, B., 1978. A palaeoecological study of Holocene peat bog sections in Germany and the Netherlands, based on the analysis of pollen, spores and macro- and microscopic remains of fungi, algae, cormophytes and animals. Rev. Palaeobot. Palynol. 25, 1–120.
van Geel, B., Bohncke, S.J.P., Dee, H., 1981. A palaeoecological study of an upper late Glacial and Holocene sequence from "De Borchert", the Netherlands. Rev. Palaeobot. Palynol. 31, 367–448.

van Geel, B., Hallewas, D.P., Pals, J.P., 1983. A Late Holocene deposit under the Westfriese Zeedijk near Enkhuizen (Prov. of Noord-Holland, the Netherlands): Palaeoecological and archaeological aspects. Rev. Palaeobot. Palynol. 38, 269–335.

van Geel, B., Coope, G.R., van der Hammen, T., 1989. Palaeoecology and stratigraphy of the lateglacial type section at Usselo (the Netherlands). Rev. Palaeobot. Palynol. 60, 25–129.

Van Strydonck, M., Van der Borg, K., 1990-1991. The construction of a preparation line for AMS-targets at the Royal Institute for Cultural Heritage Brussels. Bulletin of the Royal Institute for Cultural Heritage 23, 228–234.

Vandendriessche, H., Guéret, C., Aluwé, K., Messiaen, L., Cruz, F., Storme, A., Allemeersch, L., Sergant, J., Crombé, Ph., 2019. Bulletin de la Société Préhistorique Française (in press). Deux millénaires d'occupations mésolithiques au bord de l'Escaut à Kerkhove (Belgique) : premier compte-rendu de l'industrie lithique et des restes fauniques..

Verbruggen, C., Denys, L., Kiden, P., 1996. Belgium. In: Berglund, B.E., Birks, H.J.B., Ralska-Jasiewiezowa, M., Wright, H.E. (Eds.), Palaeoecological Events during the Last 15000 Years: Regional Syntheses of Palaeoecological Studies of Lakes and Mires in Europe. John Wiley & Sons, Chichester, pp. 553–574.

Villa, P., 1982. Conjoinable pieces and site formation processes. Am. Antiq. 47, 276–290.

Villagran, X., Huisman, H., Mentzer, S.M., et al., 2017. Bone and other skeletal tissues. In: Nicosia, C., Stoops, G. (Eds.), Archaeological Soil and Sediment Micromorphology. John Wiley & Sons Ltd, Chichester, pp. 11–38.

Zolitschka, B., 1992. Human history recorded in the annually laminated sediments of Lake Holzmaar. Eifel Mountains, Germany. Special Paper, Geological Survey of Finland 14, 17–24.